HHS Public Access

Author manuscript

Mol Cell Neurosci. Author manuscript; available in PMC 2016 September 01.

Published in final edited form as:

Mol Cell Neurosci. 2015 September ; 68: 272–283. doi:10.1016/j.mcn.2015.08.008.

The tumor suppressor HHEX inhibits axon growth when prematurely expressed in developing central nervous system neurons

Matthew T Simpson[a,*], **Ishwariya Venkatesh**[a,*], **Ben L Callif**[a], **Laura K Thiel**[a], **Denise M Coley**[a], **Kristen N Winsor**[a], **Zimei Wang**[a], **Audra A Kramer**[a], **Jessica K Lerch**[b], and **Murray G Blackmore**[a]

[a]Department of Biomedical Sciences, Marquette University, 53201

[b]The Center for Brain and Spinal Cord Repair and the Department of Neuroscience, The Ohio State University, 43210

Abstract

Neurons in the embryonic and peripheral nervous system respond to injury by activating transcriptional programs supportive of axon growth, ultimately resulting in functional recovery. In contrast, neurons in the adult central nervous system (CNS) possess a limited capacity to regenerate axons after injury, fundamentally constraining repair. Activating pro-regenerative gene expression in CNS neurons is a promising therapeutic approach, but progress is hampered by incomplete knowledge of the relevant transcription factors. An emerging hypothesis is that factors implicated in cellular growth and motility outside the nervous system may also control axon growth in neurons. We therefore tested sixty-nine transcription factors, previously identified as possessing tumor suppressive or oncogenic properties in non-neuronal cells, in assays of neurite outgrowth. This screen identified YAP1 and E2F1 as enhancers of neurite outgrowth, and PITX1, RBM14, ZBTB16, and HHEX as inhibitors. Follow-up experiments focused on the tumor suppressor HHEX, one of the strongest growth inhibitors. HHEX is widely expressed in adult CNS neurons, including corticospinal tract neurons after spinal injury, but is present in only trace amounts in immature cortical neurons and adult peripheral neurons. HHEX overexpression in early postnatal cortical neurons reduced both initial axonogenesis and the rate of axon elongation, and domain deletion analysis strongly implicated transcriptional repression as the underlying mechanism. These findings suggest a role for HHEX in restricting axon growth in the developing CNS, and substantiate the hypothesis that previously identified oncogenes and tumor suppressors can play conserved roles in axon extension.

Corresponding Author: Murray G. Blackmore, Department of Biomedical Sciences, Marquette University, Milwaukee, WI, 53201, USA. Phone: (1) 414 288-4532, murray.blackmore@marquette.edu.
*These authors contributed equally

Conflict of Interest: None

Introduction

In contrast to the peripheral nervous system (PNS) and the developing central nervous system (CNS), axons in the mature CNS generally fail to regenerate after injury. While external inhibitory factors contribute (Case and Tessier-Lavigne, 2005 ; Yiu and He, 2006), a major reason for regenerative failure is a loss of growth ability that is intrinsic to CNS neurons (Goldberg et al., 2002; Blackmore and Letourneau, 2006; Sun and He, 2010). Intervening in the CNS cell body response, either by increasing pro-regenerative gene expression or eliminating growth-inhibitory gene expression, has emerged as a promising strategy to promote axon growth (Park et al., 2008; Moore et al., 2009; Liu et al., 2010b; Blackmore et al., 2012). Given the substantial amount and diversity of cellular material needed for axon growth, it is probable that multiple targets must be altered for optimal regeneration (Sun et al., 2011). Thus transcription factors (TFs), which coordinate the expression of multiple genes, are well suited to have a profound effect on axonal growth (Moore and Goldberg, 2011; Patodia and Raivich, 2012). A number of TFs have been identified that regulate axon regeneration, but our understanding remains incomplete and additional transcriptional regulators of axon growth almost certainly await discovery (Moore and Goldberg, 2011).

It has been proposed that cellular growth mechanisms present in replicating cells outside the nervous system are conserved in post-mitotic neurons and may play key roles in axon growth (Park et al., 2008). Tumor-suppressive factors that prevent aberrant proliferation in dividing cells may act to restrict axon growth in neurons, whereas factors with oncogenic properties may act to promote axon growth (Pomerantz and Blau, 2013). Supporting this concept, signaling pathways involved in cancer progression have been found to affect neurite outgrowth (Buchser et al., 2010), most notably the mTOR pathway (Park et al., 2008) and the oncogene MYC (Belin et al., 2015). Furthermore, TFs such as KLF family members and Sox11, shown recently to promote CNS axon regeneration, are also well-studied in cancer biology (Blackmore et al., 2012; Wang et al., 2015). These findings suggest that additional transcription factors, identified previously as displaying oncogenic or tumor suppressive properties in mitotically active cells, may regulate axon extension in neurons.

To test this hypothesis we adopted a high content screening strategy in which 69 TFs, implicated previously in cancer progression, were overexpressed in assays of neurite outgrowth. Nine of these TFs were found to significantly alter neurite length, of which a tumor suppressor called Hematopoietically Expressed Homeobox (HHEX) was among the most consistent and potent growth inhibitors. In follow-up experiments we confirmed strong suppression of axon growth by HHEX without a corresponding decrease in cell viability. Moreover, although HHEX has previously been described only in non-neuronal tissues, we show expression of HHEX in the CNS that is widespread and specific to neurons. In contrast we detected only low levels of HHEX in early postnatal CNS and adult PNS neurons, and found that forced elevation of HHEX expression reduces axon growth ability. Overall these data substantiate the mechanistic link between axon growth and general cellular growth at the level of transcriptional control, and suggest the tumor suppressor HHEX may function as a novel transcriptional inhibitor of axon growth in the CNS.

Methods

Cloning and Plasmid Preparation

For screening and cell viability experiments, DNA was prepared (QIAprep Spin Miniprep Kit, Qiagen 27106) from glycerol stocks of NIH Mammalian Genome Collection in pSPORT6-CMV expression vectors (Open Biosystems, ThermoFisher, Huntsville, Alabama) (Gerhard et al., 2004). To create constructs for domain mutation analysis, a CAMKIIa promoter sequence (Zhang et al., 2007), Addgene #20944)) replaced the original CMV in pAAV-EBFP-2A-mCherry backbone (described previously, (Blackmore et al., 2012)), generating pAAV-CAMKIIa-EBFP-2A-mCherry. Next, a Histone-2B sequence ((Kita-Matsuo et al., 2009) Addgene #21217)) was inserted 5' to mCherry. cDNA encoding human HHEX (Accession BC050638) was purchased from Open Biosystems. The open reading frame (aa 1–270) was PCR-amplified and used to replace EBFP, creating CAMKIIa-HHEX-2A-H2B-mCherry. To create additional constructs, full length HHEX was replaced with amino acids 137–270 (Homeodomain and Activation domain, HHEX-ΔN), HHEX-ΔN fused to an Engrailed domain, as described in (Blackmore et al., 2012), or amino acids 1–210 (repression domain and homeodomain, HHEX-ΔC). DNA was prepared by EndoFree Plasmid Maxi Kit (Qiagen 12362) and diluted to 1μg/μl in endotoxin-free TE buffer.

Cortical cell dissociation, transfection, and culture

All animal procedures were approved by the Marquette University Institutional Animal Care and Use Committee. Cortical neurons were prepared from Sprague Dawley rat pups (Harlan) and transfected as in (Blackmore et al., 2010). Briefly, early postnatal (P3-P5) frontal cortices were placed in ice-cold Hibernate E (Life Technologies A12476-01), their meninges removed, minced finely and transferred into 10ml dissociation media for 30 minutes at 37°C with constant shaking (HibernateE containing 20U/ml papain (Worthington 3126) and 2.5μg/ml DNAse (Sigma D4527)). Cells were then rinsed with Hibernate E+ 2% SM1, gently triturated three times, rinsed in Hibernate E (no SM1), and incubated 30 minutes at 37°C with constant shaking in 10ml trypsin solution (Hibernate E containing 0.25% trypsin (Invitrogen/Gibco 15090-046) and 2.5μg/ml DNAse (Sigma D4527)). Cells were pelleted, washed with Hibernate E+ 2% SM1, and triturated three times in 1.5ml Hibernate E+ 2% SM1 containing 2μl DNAse (Sigma D4527). The suspension settled for two minutes and the supernatant was collected; the process was repeated until no cell clumps were visible. Collected cells were washed and resuspended in 6–7ml Hibernate E, typically yielding 2 million cells/ml. For transfection, cortical neurons were pelleted and resuspended to 2×10^6 cells/ml in Internal Neuronal Buffer (INB) (KCl 135mM, $CaCl_2$ 0.2mM, $MgCl_2$ 2mM, HEPES 10mM, EGTA 5mM, pH 7.3). 25μl were placed into wells of a 96-well electroporation plate (BTX Harvard Apparatus 45-0450) and mixed with 25μl of INB containing 1μg EGFP plasmid and 4μg test plasmid. A 350V, 300μs pulse was delivered to each well by an ECM square wave pulse generator (Harvard Apparatus ECM-830) attached to a plate handler (BTX Harvard Apparatus HT-200). 100μl of Hibernate E was added to each well following electroporation. For cell culture, 10,000 cells/well were placed in 24-well plates (Greiner Bio-One 662160) pre-coated with 100μg/ml Poly-D-Lysine hydrobromide (Sigma P7886) (>12 hours, 37°C), followed by 10μg/ml laminin (Sigma L2020) (>2 hours, 37°C). For inhibitory substrates, 25μg/ml Chondroitin Sulfate

Proteoglycans (Millipore CC117) were added to 10μg/ml laminin and incubated concurrently with laminin alone treatments. Cells were maintained at 37°C, 5% CO_2 in Enriched Neurobasal (ENB) media, modified from (Meyer-Franke et al., 1995), consisting of Neurobasal A (Invitrogen 10888-022), 50X NeuronCult SM1 Neuronal Supplement (Stemcell Technologies 5711), 1mM sodium pyruvate (Invitrogen 11360-070), 2mM GlutaMAX (Invitrogen/Gibco 35050-061), 50U/ml Penicillin-Streptomycin (Invitrogen 15070-063), 5μM Forskolin (Sigma F6886).

Sensory cell dissociation, transfection, and culture

Dorsal root ganglia neurons (DRGs) were isolated from freshly euthanized mice and digested with a solution of collagenase (0.5mg/mL, Invitrogen 17105-041) and dispase (10mg/mL, Invitrogen 17100) at 37 degrees for 40 minutes. Cells were brought to single suspension with pipette trituration and then pelleted at 80G for 5 minutes. The cell pellet was resuspended in the P3 Primary Cell Nucleofector kit solution (Lonza CC-4461) and approximately 20,000 DRG neurons were transfected with 1μg of EBFP-2A-H2B-mCherry or HHEX-2A-H2B-mCherry plasmid DNA using the CA-138 program on the 4D-Nucleofector™ System (Lonza). After transfection 80uL of warm PNGM™ Primary Neuron Growth Medium (Lonza CC-4461) was added to each electroporation well. The entire resulting cell solution was placed into a single well of a 24-well tissue culture plate (Corning). After 72h, cells were trypsinized, pelleted at 900G for 3 minutes, and then resuspended in 200uL of warm media. The cell suspension was divided between two wells in a 24-well tissue culture dish. 15h after replating, the cells were fixed and immunostained with a neuronal specific tubulin rabbit polyclonal antibody (1:2000, Sigma T2200) followed by secondary application of Alexa Fluor® 555 dye (Life Technologies A-21430) and Hoechst dye (0.5ug/mL, Sigma B2261) to enable nuclei detection.

Cortical Cell Culture Immunohistochemistry

Cultures were fixed in 4% paraformaldehyde (Electron Microscopy Sciences 15710) for 30 minutes at room temperature, rinsed five times, blocked and permeabilized (PBS, 20% goat serum (Invitrogen 16210-064), 0.2% Triton X-100 (G-Biosciences 786-513) for 30 minutes at room temperature, and incubated in primary antibody solution (PBS, 10% goat serum, 0.2% Triton X-100, Primary antibodies: Rabbit anti-βIII-tubulin (1:500, Sigma T2200), Mouse anti-Tau-1 (1:1000, Millipore MAB3420), Rabbit anti-MAP2 (1:2000, Millipore AB5622), Mouse anti-HHEX (1:200, Sigma SAB1403914)) (overnight, 4°C). After five washes, cultures were incubated in secondary antibody solution containing DAPI nuclear stain (PBS, 10% goat serum, 0.2% Triton X-100, 300nM DAPI, dilactate (Molecular Probes D3571) Secondary antibodies: Alexa Flour 647 goat anti-rabbit IgG (1:500, Invitrogen A21245), Alexa Fluor 488 goat anti-mouse IgG (1:500, Invitrogen A11001)) for 2 hours at room temperature. Plates were washed five times, and left in 1ml PBS for imaging.

Cortical and DRG Tissue Staining

Adult brains were snap frozen, cryosectioned into 20μm sections, post-fixed in 4% PFA (20 minutes, room temperature), blocked (1 hour, room temperature), and incubated in primary antibody solution (Primary antibodies: anti-HHEX (1:100, Sigma SAB1403914, LSBio LSB3077), anti-NeuN (1:100, MAB377A5)) overnight at 4°C. After five washes with PBS,

sections were incubated in secondary antibody solution (2 hours, room temperature), and stained with 300 nM DAPI (20 minutes, room temperature). Slides were washed with PBS three times and mounted with Fluoro-gel (Electron Microscopy sciences 1798510). CST retrograde labeling was performed on injured animals as in (Wang et al., 2015). Briefly, a 0.85mm deep lesion was made 1mm to the left of the midline between C4/C5. 1μl CTB-Alexafluor 647 (Life Technologies C-34778) was injected at C4/C5 seven days prior to sacrifice and snap freezing.

Imaging and Quantification of Neurite Length

For neurite outgrowth assays, Cellomics Cell Insight NXT (Thermo Scientific) acquired images of 3 channels: nuclei (DAPI), neurite staining (βIII-tubulin), and reporter (EGFP), and Cellomics Scan v6.4.0 (Thermo Scientific) traced neurites and quantified reporter intensity. Average total neurite length was quantified for the 10% of cells with greatest EGFP intensity per plate (n>100 cells per treatment). Average neurite length was normalized to mCherry control for each plate. Each treatment was tested at least three times; those that differed significantly from mCherry control were flagged as hit genes (*p<.05 ANOVA with post-hoc Dunnett's). For axon growth and differentiation assays, a fluorescent inverted microscope was used to identify mCherry+ MAP2+ cells as transfected neurons. Axons were identified by Tau-1 staining, and hand traced using NIS-Elements Basic Research software. Axon length for neurons with an axon and percentage of neurons with an axon were quantified for n=75 cells per treatment. Statistical analysis was paired t-test using Graphpad Prism Software.

For DRG neurite outgrowth assays, a Cellomics ArrayScanXTI (Thermo Scientific) acquired images in 3 channels: nuclei (Hoechst), neurite staining (βIII-tubulin), and reporter (mCherry), and the Neuronal Profiling v4.1 algorithm (Thermo Scientific) traced neurites and quantified reporter intensity. Cells were considered mCherry+ when the pixel intensity in the cell reached 2 standard deviations above the mean intensity for mCherry in non-transfected control wells. Average neurite length was normalized to EBFP-2A-H2B-mCherry for each plate. The experiment was repeated three times. Statistical analysis was paired t-test using Graphpad Prism Software.

Cell Survival Assay

Cortical neurons were transfected and cultured as previously described, using HHEX as the test gene and an EBFP-2A-mCherry reporter in place of EGFP. After one day in culture, 1μM staurosporine toxin (Sigma S5921) was added to a subset of EBFP-2A-mCherry wells. The following day media was replaced with either 0.05μM Calcein AM (Life Technologies C3099), or 0.01μM Yo-Pro-1-Iodide (Life Technologies Y3603), both in PBS and containing 1μg/ml Hoechst 33342 (Molecular Probes H1399), and incubated (30 minutes, 37°C). Cellomics Cell Insight NXT (Thermo Scientific) acquired images for three channels: nuclear (Hoechst 33342), cell survival stain (Calcein AM or Yo-Pro), and reporter (EBFP-2A-mCherry); compartmental analysis quantified intensities for each channel, and data were exported to Excel for analysis. The percentage of surviving cells (Hoechst+/Calcein AM+) and the percentage of apoptotic cells (Hoechst+/Yo-Pro-1-Iodide+) was quantified in five

independent experiments. Statistical analysis was by ANOVA with post-hoc Dunnett's was performed using Graphpad Prism Software.

Western Blotting

Lysates for western blotting were prepared from HEK293 cells that were transfected with either EBFP-2A-H2B-mCherry or HHEX-2A-H2B-mCherry plasmids according to manufacturer's instructions (Lipofectamine 2000, Invitrogen 11668-027). Two days post incubation, cells were lysed using 200μl lysis buffer (150Mm Sodium Chloride, 1.0% Triton-X 100, 0.5% Sodium deoxycholate, 0.1% SDS, 50Mm Tris with protease inhibitors according to manufacturer's instructions (Roche 5892791001)), and cell debris was removed through centrifugation at 4 degrees for 15 mins at 21,000 rcf. P3 cortex, adult cortex and adult DRGs tissues were collected into 200–500μl lysis buffer, and lysed using a homogenizer (VWR KT885450-0020), incubated on ice for 30 mins and cell debris was removed through centrifugation at 4 degrees. Protein concentration was estimated using the BCA method. A portion of the lysate (10–40 μg of protein) was fractionated by SDS-polyacrylamide gel electrophoresis (SDS-PAGE), and the separated proteins were transferred to a PVDF membrane. Specific antibodies (Sigma SAB1403914; LSBio LSB3077; 1:1000 dilution) were used to probe for HHEX protein. Immune complexes were detected with suitable secondary antibodies and chemiluminescence reagents (ThermoScientific). β-actin primary antibody (ab6276, 1:2500 dilution) was used to ensure equal gel loading and transfer.

Results

High content screening of cancer related transcription factors

We first used existing datasets to examine the potential overlap between TFs implicated in cancer biology with TFs linked to axon growth. Using the Gene Ranker tool maintained by the Memorial Sloan Kettering Cancer Center, we acquired a list of 1,258 genes that are strongly correlated with and/or functionally linked to oncogenesis or tumor suppression. This list contained 254 TFs, as defined by Gene Ontology terms DNA Binding and Regulation of Transcription, DNA Template. Of these, 166 TFs are expressed in the adult and/or developing cortex according to the Allen Brain Atlas (Supplementary Table 1). Intriguingly, these 166 cancer-related TFs included many genes that are already known to regulate axon growth, including 9 out of 10 factors discussed in a recent review of the transcriptional control of axon growth (ATF3, CREB, JUN, KLF4 and −6, NFKB1, SNON, the SOXC family, STAT3, and p53/TP53) (Gao et al., 2004; Qiu et al., 2005; Stegmuller et al., 2006; Gallagher et al., 2007; Seijffers et al., 2007; Jankowski et al., 2009; Moore et al., 2009; Tedeschi et al., 2009; Lerch et al., 2014; Wang et al., 2015).This high degree of overlap supports the notion of common transcriptional mechanisms that influence growth across diverse cell types, and raised the question of whether other cancer-implicated TFs on the list, many of which are unstudied in a neuronal context, might also act as regulators of axon growth.

We therefore used an established high content screening approach to quantify how cancer-related TFs affected neurite outgrowth when expressed in cortical neurons (Moore et al.,

2009; Blackmore et al., 2010; Lerch et al., 2014). Sixty-nine cancer-related TFs were examined. Importantly, this subset was an effectively random sample based on availability in pre-made expression libraries (Open Biosystems), and not selected by user prioritization. Postnatal rat cortical neurons were co-transfected with plasmid DNA encoding test genes and a fluorescent reporter plasmid and then cultured on laminin substrate. Two days later, automated microscopy (ThermoScientific CellInsight Nxt) quantified neurite outgrowth from cells identified as neurons through βIII tubulin immunostaining (Fig. 1B) and positive for transfection through expression of EGFP reporter (Fig. 1C). Each gene was tested in three independent experiments, and neurite lengths were normalized to mCherry control (Supplementary Table 1). The set of "cancer" genes included JUN, a known promoter of neurite growth, as well as KLF4 and KLF6, shown previously to inhibit and promote neurite growth, respectively (Moore et al., 2009; Blackmore et al., 2010; Lerch et al., 2014). These genes therefore functioned as positive controls. As expected, KLF4 significantly reduced (73.3% +/− 3.7%, $p<0.01$) and KLF6 and JUN expression significantly increased (125.8% +/− 5.6%, 126.2% +/− 6.9%, $p<0.01$) neurite lengths, confirming the screen's ability to detect TF-evoked changes in neurite length. Notably, in addition to the controls, 6 candidate genes significantly altered neurite lengths, with 2 acting as growth enhancers and 4 as suppressors (Fig. 1E). In summary, nearly 15% of candidate TFs, selected on the basis of their involvement in cellular growth outside the nervous system, displayed an ability to modulate neurite outgrowth in primary neurons.

HHEX inhibits axonogenesis without affecting viability

The homeodomain factor HHEX emerged from the initial screening experiment as one of the most potent and consistent inhibitors of neurite outgrowth, and was prioritized for additional analysis. To better characterize the effects of HHEX on neuronal morphology we performed a time-course experiment with axon-specific Tau1 antibodies (Fig. 2). Postnatal cortical neurons were transfected with either HHEX plasmid DNA or EBFP control, and axon formation and length were quantified by hand tracing of Tau1-positive neurites. About 35% of control-transfected neurons extended an axon (Tau1+ process) within 24 hours of plating, and the percent of axon-bearing neurons increased steadily to a plateau of about 90% by three days *in vitro* (DIV; Fig. 2C). In contrast, within 24 hours of plating only 21% of HHEX-transfected neurons extended a Tau+ axon (Fig. 2C), and the percent of axon-bearing HHEX-transfected neurons never rose above 45%. These data confirm that HHEX expression interferes with axonogenesis.

To determine whether HHEX also affects the rate of extension of existing axons we hand-traced Tau1+ processes at 2 and 3DIV; quantification at 4DIV was prevented by overgrowth of axons that prevented clear discrimination of the cell of origin. At 2DIV, axon length in HHEX-expressing neurons was 44% lower than control (161μm +/− 26.7μm SEM versus 284.4μm +/− 36.8μm SEM; $p<0.01$, paired T-test) (Fig. 2D). Over the next 24 hours, control neurons increased average axon lengths to 653.3μm +/− 76.4μm SEM (an average net addition of 368.9μm), while HHEX-expressing neurons increased to 357.5μm +/− 40.0μm SEM, (an average net addition of 195.5μm). These data indicate that HHEX expression does not simply delay axon formation, but also slows net axon growth between 2DIV and 3DIV. Consistent with this, a time-course analysis using automated tracing showed that HHEX and

EBFP-transfected neurons displayed similar neurite lengths at the one day time-point, but that the subsequent daily increases in neurite length were more than 50% lower in HHEX-expressing neurons (Supplemental Fig. 1). Thus HHEX expression also appears to decrease the rate of elongation of extant processes.

We next considered the possibility that the effect of HHEX on axon growth could be secondary to a reduction in cell viability. This issue is particularly important given the involvement of HHEX in cell proliferation in non-neuronal cells, and findings that modulation of cell cycle regulators can induce apoptosis in post-mitotic neurons (Kranenburg et al., 1996; Nguyen et al., 2002 ; Greene et al., 2004; Hoglinger et al., 2007). Cortical neurons were transfected with HHEX or EBFP control plasmid carrying mCherry reporter, and a third group of EBFP-transfected neurons were treated with the toxin staurosporine as a positive control for reduced viability. After two days in culture, a time point at which effects on axon growth are robust (Fig. 2), Cellomics image analysis quantified the percent of transfected (mCherry+) neurons that stained positively for Yo-Pro-1-Iodide or Calcein AM, indicators of apoptotic and live cells respectively (Fig. 3A–F). As expected, staurosporine elevated Yo-Pro and decreased Calcein signal, confirming the sensitivity of the assay. In contrast, HHEX-transfected neurons showed neither elevated Yo-Pro signal nor decreased Calcein compared to EBFP control (Fig. 3G). Combined, these experiments confirm that HHEX overexpression interferes with axonogenesis and slows axon elongation, without any corresponding decrease in cell viability.

Mutation analysis suggests transcriptional repression as relevant mechanism

Wild type HHEX protein is comprised of a DNA binding domain flanked by an N-terminal domain that mediates transcriptional repression (Tanaka et al., 1999), and a C-terminal domain that mediates transcriptional activation (Kasamatsu et al., 2004; Soufi and Jayaraman, 2008). Thus, depending on cellular context, HHEX can either activate or repress target genes, raising the question of which activity is relevant to the suppression of axon growth. We therefore created HHEX truncation mutants that lacked either the activation domain (HHEX-ΔC) or the repression domain (HHEX-ΔN), and tested their effects on neurite outgrowth in cortical neurons, as described above (Fig. 4). All constructs included a 2A-H2B-mCherry fluorescent reporter, allowing specific identification of transfected cells. In addition, the fluorescent reporter, as well as direct immunohistochemistry for HHEX protein, confirmed effective expression of all constructs. Removal of the repression domain, but not the activation domain, completely abolished growth inhibition, suggesting that transcriptional repression may be necessary for HHEX's effects on neurite growth (Fig. 4B). Moreover, a chimeric construct in which the endogenous HHEX N-terminal domain was replaced by an alternative Engrailed repression domain phenocopied the full length HHEX repression of neurite outgrowth. This result indicates that transcriptional repression *per se*, as opposed to a non-transcriptional activity localized to the N-terminal HHEX sequence, causes inhibition of axon growth. Combined, these data identify transcriptional repression domains as both necessary and sufficient for HHEX's inhibition of neurite growth, and suggest a model in which HHEX normally inhibits gene targets that are needed for efficient neurite extension.

HHEX is expressed in adult CNS neurons

Although CNS expression is suggested by *in situ* data from the Allen Brain Atlas, HHEX has been previously described only in hematopoietic lineages and in endoderm-derived tissues such as thyroid, pancreas, liver, and lung (Bogue et al., 2000; Soufi and Jayaraman, 2008). To establish HHEX's relevance to axon growth it is therefore essential to examine its endogenous pattern of expression in the nervous system. We first validated two anti-HHEX antibodies using HHEX-transfected HEK293 cells. As expected, control-transfected 293 cells displayed no HHEX expression by immunohistochemistry or western blotting, whereas HHEX-transfected cells showed clear signal with both antibodies (Supplemental Fig. 2). These data demonstrate the specificity of the anti-HHEX antibodies in both immunohistochemistry and western blotting experiments.

We first examined HHEX expression in the adult murine cortex by western blot, and observed a clear ~42kD band at the same position as overexpressed full-length HHEX (Fig. 5A). These data confirm expression of HHEX protein in the adult cortex. In contrast, cortex from postnatal day 3 (P3), the age at which cells were prepared for neurite outgrowth assays, did not show detectable expression of HHEX by western blotting. Consistent with this, immunohistochemistry on cultured P3 cortical neurons detected no endogenous HHEX in cells transfected with EBFP control plasmid, but did confirm the presence of HHEX protein in cells transfected with HHEX plasmid (Fig. 5B–E). Combined, these data demonstrate expression of HHEX in cortical tissue of adult but not early postnatal age.

To further explore the relationship between HHEX protein expression and neurite length we visualized HHEX protein in HHEX-transfected or EBFP-transfected control neurons while simultaneously measuring neurite lengths. Quantification of the intensity of HHEX immunohistochemistry signal in HHEX-transfected neurons showed a range of intensities above the background level in control cells, indicating variable levels of HHEX protein expression (Supplemental Fig. 3). Analysis of average neurite lengths, binned according to increasing levels of HHEX protein, confirmed a significant reduction in neurite length in neurons with elevated HHEX expression. Neurite lengths were significantly reduced in neurons with relatively modest HHEX expression, such that neurons within the second quintile of HHEX intensity were 71.2% of control length ($P<.05$, ANOVA with Dunnet's post-hoc), with neurons in the brightest HHEX quintile averaging 56.1% of control. These data confirm with direct detection that increased expression of HHEX protein in postnatal cortical neurons reduces neurite outgrowth.

To determine whether HHEX is expressed specifically in neurons in the adult brain, as opposed to other cell types, we examined murine brain sections by immunohistochemistry, using NeuN as a neuronal marker. Intriguingly, we observed a striking and complete overlap between HHEX and NeuN reactivity (Fig 5F–K). HHEX was detected in all NeuN+ nuclei examined in the forebrain, midbrain and hindbrain and was not detected in adjacent NeuN-negative nuclei, indicating expression that is widespread and highly specific to neurons. To confirm these findings we repeated the experiment with a second antibody against HHEX that was raised against a distinct epitope, with identical results (Supplemental Fig. 4). To assess HHEX expression in CNS neurons that are responding to axotomy, we performed spinal transections and injected retrograde tracers to the injury site to identify axotomized

corticospinal tract (CST) neurons. Two weeks post-injury, HHEX was readily detectable in all injured CST neurons, and the intensity of staining appeared neither elevated nor decreased (Fig. 6). These data show expression of HHEX protein in the adult CNS neurons, including CST neurons after spinal injury.

Axon growth in the adult CNS is constrained in part by inhibitory substrates such as chondroitin sulfate proteoglycans (CSPGs) (Carulli et al., 2005). We therefore explored potential interactions between CSPG substrates and HHEX expression by culturing neurons on substrates of laminin (10μg/ml) or a mixture of laminin and CSPGs (10μg/ml laminin, 25μg/ml CSPGs) and performing immunohistochemistry for HHEX. HHEX was detectable on neither substrate, and automated microscopy confirmed similar levels of HHEX signal on laminin and CSPG substrates. As a positive control the immunohistochemistry, HHEX was readily detectable in HHEX-transfected cells. (Fig. 7A–E). These data indicate that HHEX expression is insensitive to CSPG exposure.

Next, to test whether HHEX-mediated inhibition of neurite outgrowth was affected by CSPG substrates, neurons were transfected with HHEX or control plasmid and cultured on laminin or CSPG substrates. As expected, neurite outgrowth by control-transfected neurons was reduced on CSPG substrates (69.9% shorter than on laminin) (Fig. 7F). On laminin substrate, HHEX expression caused a 39% reduction in neurite length compared to mCherry control. On CSPG substrates, HHEX also reduced neurite lengths, and did so to a degree that was proportional to the effect on laminin (35% shorter than control-transfected neurons on CSPGs). Combined with the insensitivity of HHEX expression to CSPG, these data suggest that the molecular mechanisms that mediate growth inhibition by HHEX function independently of those triggered by CSPG substrates.

HHEX expression and function in peripheral neurons

We next examined HHEX expression in peripheral neurons of the dorsal root ganglia (DRG), which possess a generally higher regenerative capacity than CNS neurons. Immunohistochemistry for HHEX showed very dim signal in sections of adult DRG; as a positive control, adult cortical tissue processed in parallel and visualized with identical acquisition parameters showed bright HHEX signal (Fig. 8A, B). Similarly, western blotting in DRG tissue detected very faint size-shifted bands, but no HHEX protein in a position corresponding to overexpressed HHEX protein or to protein detected in adult cortex (Fig. 8C). Adult DRG neurons are known to extend lengthy processes when placed in culture, and this response requires extensive transcriptional changes that occur in the days after plating. We therefore performed immunohistochemistry for HHEX in DRG neurons that were transfected with EBFP-2A-H2B-mCherry control or HHEX-2A-H2B-mCherry and maintained in culture for three days (Fig 8D–G). HHEX protein was not detected in control-transfected DRG neurons, but was readily detectable in HHEX-transfected cells (Fig 8D–G). Combined, these data suggest that unlike CNS neurons, regeneration-competent PNS neurons do not express detectable amounts of HHEX protein in neither the uninjured state, nor when engaged in injury-triggered axon growth.

We therefore tested the effects of elevating full-length HHEX expression in DRG neurons. Cultured DRG neurons were transfected with plasmids encoding HHEX or EBFP,

maintained for the three days, and then replated to remove existing neurites. The amount of neurite growth generated in the subsequent 24 hours was then quantified. This paradigm avoids technical problems associated with excessive axon growth by DRG neurons during the lag between plasmid transfection and protein function. Immunohistochemistry confirmed exogenous HHEX expression (Fig. 8F, G). Compared to EBFP control, HHEX expression significantly reduced the number of neurites by 2-fold and the total length of neurites produced by DRG neurons (Fig. 9). Combined, these data demonstrate that ectopic expression of full-length HHEX, normally absent in PNS neurons, is sufficient to reduce the regenerative capacity of DRG neurons.

Discussion

This study used a screening approach to identify the homeodomain factor HHEX, previously studied as a tumor suppressor in hematopoietic and endodermal lineages, as a potent suppressor of axon growth when overexpressed in CNS neurons. Our data suggest that HHEX may act through a mechanism of transcriptional repression to reduce both axon initiation and extension, without negatively affecting cell viability. Moreover, HHEX is endogenously expressed in the nuclei of CNS neurons, including CST neurons after axotomy. In contrast, peripheral DRG neurons express much lower levels of HHEX, and forced expression of HHEX reduces DRG axon growth. Combined, the phenotypic effects and pattern of expression support the hypothesis that transcriptional repression by HHEX may limit axon growth in CNS neurons.

Transcriptional inhibition of axon growth

In contrast to HHEX, the majority of TFs that have previously been linked to axon growth appear to play pro-regenerative roles, likely by coordinating the production of multiple growth-associated proteins. Prominent examples include JUN, ATF3, KLF7, SOX11, STAT3, and CREB, all of which are active in neurons that mount successful axon regeneration but are missing or inactive in non-regenerating cell types (Gao et al., 2004; Qiu et al., 2005 ; Seijffers et al., 2007; Jankowski et al., 2009; Blackmore et al., 2012; Lerch et al., 2014). Accordingly, we and others have pursued forced expression of these TFs as a strategy to enhance axon growth (Qiu et al., 2005; Seijffers et al., 2007; Jankowski et al., 2009; Blackmore et al., 2012; Lerch et al., 2014; Wang et al., 2015). It is well appreciated, however, that regenerative ability can also be held in check by the presence of cell-intrinsic factors that limit growth potential. Thus, at the level of gene transcription, it may be necessary to complement the overexpression approach by neutralizing TFs that repress transcription by occupying pro-regenerative loci. The identity of such growth-inhibitory TFs, however, remains unclear. Members of the KLF family, notably KLF4, are likely candidates because they are expressed in poorly-regenerating CNS neurons and contribute to their low regenerative capacity (Moore et al., 2009). Whether KLF4 acts as a transcriptional repressor of pro-regenerative genes, as opposed to alternative mechanisms such as activation of growth inhibitory genes, has not been established.

In this context it is significant that the functional domain analyses suggest that HHEX inhibits axon growth through a mechanism of transcriptional repression. Although HHEX is

known to be capable of either activating or repressing target genes, the domain deletion experiments showed that a known activation domain is dispensable, and a known repression domain essential, for inhibition of neurite outgrowth. In addition, evidence that the Engrailed repression domain can effectively substitute for the endogenous HHEX repression domain makes it likely that transcriptional repression, and not an alternative function specific to the HHEX N-terminal sequence, drives inhibition of neurite growth. Direct assays of transcriptional activity (e.g. luciferase assays with promoter mutations/deletion) are needed to confirm HHEX's transcriptional mode of activity, but the experiments reported here support a working model in which HHEX transcriptionally represses gene products needed for efficient axon growth.

HHEX is relatively unstudied in the nervous system, but well characterized in other systems. HHEX functions as an essential regulator of vertebrate development, controlling hematopoietic and vascular system formation as well as formation of the vertebrate body axis early in development (Soufi and Jayaraman, 2008). HHEX is also essential for the formation and maintenance of organs derived from the foregut endoderm such as thyroid, liver and lung (Bogue et al., 2000). HHEX knockout animals die embryonically around day 12 and show anterior truncation including a lack of forebrain tissue, but this defect has been interpreted as secondary to defects in the anterior visceral endoderm signaling center (Martinez-Barbera et al., 2000; Martinez Barbera et al., 2000)

In adult mammals, we find that full length HHEX is widely expressed in neurons throughout the central nervous system, with expression localized to neuronal nuclei. Consistent with a role for HHEX in axon growth inhibition, we observe that CST neurons, which are generally refractory to regenerative axon growth, display HHEX expression after spinal injury. In contrast, HHEX appears to be much less abundant in early postnatal cortical neurons and in DRG neurons, both constitutively and during injury-triggered axon growth. When full length HHEX is overexpressed in early postnatal cortical neurons or DRG neurons, both of which are innately regeneration competent, we observe defects in both axon formation and extension. Immunohistochemistry showed that significant reductions in neurite length occurred in neurons with relatively dim immunohistochemistry HHEX signal. Although comparison between immunohistochemistry experiments must be made cautiously, it is notable that the intensity of HHEX signal that produced significant reductions in neurite length in cultured neurons appeared comparable to or dimmer than the intensity of endogenous HHEX in the adult brain. Combined, these data are consistent with the notion that endogenous HHEX expression in adult neurons may restrict axon growth.

The identity of HHEX target genes in neurons remains unclear. In various proliferative cell types, a number of genes have been shown to change in expression upon HHEX overexpression or knockdown, including ESM1, VEGF, SST, KIT, and cyclin dependent kinases and associated inhibitors (Noy et al., 2010; Shields et al., 2014; Zhang et al., 2014; Jackson et al., 2015). In the case of ESM1, VEGFR, and SST direct binding of HHEX to promoter sites has been demonstrated, whereas other gene targets may be direct or indirect (Cong et al., 2006; Noy et al., 2010; Zhang et al., 2014). In either case, the link between these known targets and the suppression of axon growth is not obvious. Intriguingly, HHEX has also been shown to inhibit the activity of JUN, a well-studied transcriptional promoter of

axon growth that we confirmed here to increase neurite length (Schaefer et al., 2001; Raivich et al., 2004; Lerch et al., 2014). HHEX was also recently shown to negatively regulate the activity of MYC, a TF implicated in cellular growth and proliferation, and very recently linked to axon regeneration in the optic system (Belin et al., 2015; Marfil et al., 2015). Determining direct and indirect gene targets of HHEX in neurons, and clarifying the potential interactions of HHEX with JUN and/or MYC in the context of axon growth, represent important directions for future research.

Oncogenes and tumor suppressors as regulators of axon growth

The general notion that intracellular factors implicated in cancer biology could regulate axon growth has been previously proposed (Park et al., 2008). Axon growth may depend on catabolic processes and cytoskeletal dynamics that contribute to cell proliferation and motility, much like what is observed in cancerous cells. Conversely, tumor suppressive molecules are in place to prevent aberrant growth upon maturation. Since many of these genes are expressed in post-mitotic neurons, it raises a possibility that the tumor suppressor genes may inhibit axonal growth and contribute to the reduced regenerative capacity observed in mature CNS neurons. In line with this, the proto-oncogene JUN drives regenerative axon growth (Raivich et al., 2004; Lerch et al., 2014) whereas the tumor suppressor KLF4 restricts axon growth (Moore et al., 2009).

We therefore undertook a systematic evaluation of this idea by selecting factors based on their tumor suppressor/oncogenic properties and examining their effects on neurite growth. Approximately 13% (9/69) of the factors tested altered neurite growth, as compared to about 2% (8/428) in a previous screen using similar techniques but which focused on genes that are developmentally regulated (Blackmore et al., 2010). This relatively high hit rate corroborates the concept that mechanisms driving cellular growth and motility are conserved across cell types. Intriguingly, the two TFs that emerged as growth promoting in the screen (E2F1 and YAP1) are generally considered oncogenic (Alonso et al., 2008; Liu et al., 2010a) , whereas the four growth-suppressors (HHEX, PITX1, RBM14, and ZBTB16) have been described as tumor suppressive (Kolfschoten et al., 2005; Kang et al., 2008; Soufi and Jayaraman, 2008; Suliman et al., 2012). Although it should be noted that factors cannot always be cleanly classified due to conflicting findings in different cell types (George et al., 2003), the screen results support an overall correlation between oncogenesis and axon growth and tumor suppression with growth inhibition. Thus further study of factors implicated in cancer biology may be a productive means to identify new regulators of axon growth.

Supplementary Material

Refer to Web version on PubMed Central for supplementary material.

Acknowledgments

This work was supported by the Craig H. Neilsen Foundation, the International Spinal Research Trust, and the Bryon Riesch Paralysis Foundation.

REFERENCES

Alonso MM, Alemany R, Fueyo J, Gomez-Manzano C. E2F1 in gliomas: a paradigm of oncogene addiction. Cancer Lett. 2008; 263:157–163. [PubMed: 18334281]

Belin S, Nawabi H, Wang C, Tang S, Latremoliere A, Warren P, Schorle H, Uncu C, Woolf CJ, He Z, Steen JA. Injury-induced decline of intrinsic regenerative ability revealed by quantitative proteomics. Neuron. 2015; 86:1000–1014. [PubMed: 25937169]

Blackmore M, Letourneau PC. Changes within maturing neurons limit axonal regeneration in the developing spinal cord. J Neurobiol. 2006; 66:348–360. [PubMed: 16408302]

Blackmore MG, Moore DL, Smith RP, Goldberg JL, Bixby JL, Lemmon VP. High content screening of cortical neurons identifies novel regulators of axon growth. Mol Cell Neurosci. 2010; 44:43–54. [PubMed: 20159039]

Blackmore MG, Wang Z, Lerch JK, Motti D, Zhang YP, Shields CB, Lee JK, Goldberg JL, Lemmon VP, Bixby JL. Kruppel-like Factor 7 engineered for transcriptional activation promotes axon regeneration in the adult corticospinal tract. Proc Natl Acad Sci U S A. 2012; 109:7517–7522. [PubMed: 22529377]

Bogue CW, Ganea GR, Sturm E, Ianucci R, Jacobs HC. Hex expression suggests a role in the development and function of organs derived from foregut endoderm. Dev Dyn. 2000; 219:84–89. [PubMed: 10974674]

Buchser WJ, Slepak TI, Gutierrez-Arenas O, Bixby JL, Lemmon VP. Kinase/phosphatase overexpression reveals pathways regulating hippocampal neuron morphology. Mol Syst Biol. 2010; 6:391. [PubMed: 20664637]

Carulli D, Laabs T, Geller HM, Fawcett JW. Chondroitin sulfate proteoglycans in neural development and regeneration. Curr Opin Neurobiol. 2005; 15:116–120. [PubMed: 15721753]

Case LC, Tessier-Lavigne M. Regeneration of the adult central nervous system. Curr Biol. 2005; 15:R749–R753. [PubMed: 16169471]

Cong R, Jiang X, Wilson CM, Hunter MP, Vasavada H, Bogue CW. Hhex is a direct repressor of endothelial cell-specific molecule 1 (ESM-1). Biochem Biophys Res Commun. 2006; 346:535–545. [PubMed: 16764824]

Gallagher D, Gutierrez H, Gavalda N, O'Keeffe G, Hay R, Davies AM. Nuclear factor-kappaB activation via tyrosine phosphorylation of inhibitor kappaB-alpha is crucial for ciliary neurotrophic factor-promoted neurite growth from developing neurons. J Neurosci. 2007; 27:9664–9669. [PubMed: 17804627]

Gao Y, Deng K, Hou J, Bryson JB, Barco A, Nikulina E, Spencer T, Mellado W, Kandel ER, Filbin MT. Activated CREB is sufficient to overcome inhibitors in myelin and promote spinal axon regeneration in vivo. Neuron. 2004; 44:609–621. [PubMed: 15541310]

George A, Morse HC 3rd, Justice MJ. The homeobox gene Hex induces T-cell-derived lymphomas when overexpressed in hematopoietic precursor cells. Oncogene. 2003; 22:6764–6773. [PubMed: 14555989]

Gerhard DS, et al. The status, quality, and expansion of the NIH full-length cDNA project: the Mammalian Gene Collection (MGC). Genome Res. 2004; 14:2121–2127. [PubMed: 15489334]

Goldberg JL, Klassen MP, Hua Y, Barres BA. Amacrine-signaled loss of intrinsic axon growth ability by retinal ganglion cells. Science. 2002; 296:1860–1864. [PubMed: 12052959]

Greene LA, Biswas SC, Liu DX. Cell cycle molecules and vertebrate neuron death: E2F at the hub. Cell Death Differ. 2004; 11:49–60. [PubMed: 14647236]

Hoglinger GU, Breunig JJ, Depboylu C, Rouaux C, Michel PP, Alvarez-Fischer D, Boutillier AL, Degregori J, Oertel WH, Rakic P, Hirsch EC, Hunot S. The pRb/E2F cell-cycle pathway mediates cell death in Parkinson's disease. Proc Natl Acad Sci U S A. 2007; 104:3585–3590. [PubMed: 17360686]

Jackson JT, Nasa C, Shi W, Huntington ND, Bogue CW, Alexander WS, McCormack MP. A crucial role for the homeodomain transcription factor Hhex in lymphopoiesis. Blood. 2015; 125:803–814. [PubMed: 25472970]

Jankowski MP, McIlwrath SL, Jing X, Cornuet PK, Salerno KM, Koerber HR, Albers KM. Sox11 transcription factor modulates peripheral nerve regeneration in adult mice. Brain Res. 2009; 1256:43–54. [PubMed: 19133245]

Kang YK, Schiff R, Ko L, Wang T, Tsai SY, Tsai MJ, O'Malley BW. Dual roles for coactivator activator and its counterbalancing isoform coactivator modulator in human kidney cell tumorigenesis. Cancer Res. 2008; 68:7887–7896. [PubMed: 18829545]

Kasamatsu S, Sato A, Yamamoto T, Keng VW, Yoshida H, Yamazaki Y, Shimoda M, Miyazaki J, Noguchi T. Identification of the transactivating region of the homeodomain protein, hex. J Biochem. 2004; 135:217–223. [PubMed: 15047723]

Kita-Matsuo H, Barcova M, Prigozhina N, Salomonis N, Wei K, Jacot JG, Nelson B, Spiering S, Haverslag R, Kim C, Talantova M, Bajpai R, Calzolari D, Terskikh A, McCulloch AD, Price JH, Conklin BR, Chen HS, Mercola M. Lentiviral vectors and protocols for creation of stable hESC lines for fluorescent tracking and drug resistance selection of cardiomyocytes. PLoS One. 2009; 4:e5046. [PubMed: 19352491]

Kolfschoten IG, van Leeuwen B, Berns K, Mullenders J, Beijersbergen RL, Bernards R, Voorhoeve PM, Agami R. A genetic screen identifies PITX1 as a suppressor of RAS activity and tumorigenicity. Cell. 2005; 121:849–858. [PubMed: 15960973]

Kranenburg O, van der Eb AJ, Zantema A. Cyclin D1 is an essential mediator of apoptotic neuronal cell death. EMBO J. 1996; 15:46–54. [PubMed: 8598205]

Lerch JK, Martinez-Ondaro YR, Bixby JL, Lemmon VP. cJun promotes CNS axon growth. Mol Cell Neurosci. 2014; 59:97–105. [PubMed: 24521823]

Liu AM, Xu MZ, Chen J, Poon RT, Luk JM. Targeting YAP and Hippo signaling pathway in liver cancer. Expert Opin Ther Targets. 2010a; 14:855–868. [PubMed: 20545481]

Liu K, Lu Y, Lee JK, Samara R, Willenberg R, Sears-Kraxberger I, Tedeschi A, Park KK, Jin D, Cai B, Xu B, Connolly L, Steward O, Zheng B, He Z. PTEN deletion enhances the regenerative ability of adult corticospinal neurons. Nat Neurosci. 2010b; 13:1075–1081. [PubMed: 20694004]

Marfil V, Blazquez M, Serrano F, Castell JV, Bort R. Growth-promoting and tumourigenic activity of c-Myc is suppressed by Hhex. Oncogene. 2015; 34:3011–3022. [PubMed: 25220416]

Martinez-Barbera JP, Rodriguez TA, Beddington RS. The homeobox gene Hesx1 is required in the anterior neural ectoderm for normal forebrain formation. Dev Biol. 2000; 223:422–430. [PubMed: 10882526]

Martinez Barbera JP, Clements M, Thomas P, Rodriguez T, Meloy D, Kioussis D, Beddington RS. The homeobox gene Hex is required in definitive endodermal tissues for normal forebrain, liver and thyroid formation. Development. 2000; 127:2433–2445. [PubMed: 10804184]

Meyer-Franke A, Kaplan MR, Pfrieger FW, Barres BA. Characterization of the signaling interactions that promote the survival and growth of developing retinal ganglion cells in culture. Neuron. 1995; 15:805–819. [PubMed: 7576630]

Moore DL, Goldberg JL. Multiple transcription factor families regulate axon growth and regeneration. Dev Neurobiol. 2011; 71:1186–1211. [PubMed: 21674813]

Moore DL, Blackmore MG, Hu Y, Kaestner KH, Bixby JL, Lemmon VP, Goldberg JL. KLF family members regulate intrinsic axon regeneration ability. Science. 2009; 326:298–301. [PubMed: 19815778]

Nguyen MD, Mushynski WE, Julien JP. Cycling at the interface between neurodevelopment and neurodegeneration. Cell Death Differ. 2002; 9:1294–1306. [PubMed: 12478466]

Noy P, Williams H, Sawasdichai A, Gaston K, Jayaraman PS. PRH/Hhex controls cell survival through coordinate transcriptional regulation of vascular endothelial growth factor signaling. Mol Cell Biol. 2010; 30:2120–2134. [PubMed: 20176809]

Park KK, Liu K, Hu Y, Smith PD, Wang C, Cai B, Xu B, Connolly L, Kramvis I, Sahin M, He Z. Promoting axon regeneration in the adult CNS by modulation of the PTEN/mTOR pathway. Science. 2008; 322:963–966. [PubMed: 18988856]

Patodia S, Raivich G. Downstream effector molecules in successful peripheral nerve regeneration. Cell Tissue Res. 2012; 349:15–26. [PubMed: 22580509]

Pomerantz JH, Blau HM. Tumor suppressors: enhancers or suppressors of regeneration? Development. 2013; 140:2502–2512. [PubMed: 23715544]

Qiu J, Cafferty WB, McMahon SB, Thompson SW. Conditioning injury-induced spinal axon regeneration requires signal transducer and activator of transcription 3 activation. J Neurosci. 2005; 25:1645–1653. [PubMed: 15716400]

Raivich G, Bohatschek M, Da Costa C, Iwata O, Galiano M, Hristova M, Nateri AS, Makwana M, Riera-Sans L, Wolfer DP, Lipp HP, Aguzzi A, Wagner EF, Behrens A. The AP-1 transcription factor c-Jun is required for efficient axonal regeneration. Neuron. 2004; 43:57–67. [PubMed: 15233917]

Schaefer LK, Wang S, Schaefer TS. Functional interaction of Jun and homeodomain proteins. J Biol Chem. 2001; 276:43074–43082. [PubMed: 11551904]

Seijffers R, Mills CD, Woolf CJ. ATF3 increases the intrinsic growth state of DRG neurons to enhance peripheral nerve regeneration. J Neurosci. 2007; 27:7911–7920. [PubMed: 17652582]

Shields BJ, Alserihi R, Nasa C, Bogue C, Alexander WS, McCormack MP. Hhex regulates Kit to promote radioresistance of self-renewing thymocytes in Lmo2-transgenic mice. Leukemia. 2014

Soufi A, Jayaraman PS. PRH/Hex: an oligomeric transcription factor and multifunctional regulator of cell fate. Biochem J. 2008; 412:399–413. [PubMed: 18498250]

Stegmuller J, Konishi Y, Huynh MA, Yuan Z, Dibacco S, Bonni A. Cell-intrinsic regulation of axonal morphogenesis by the Cdh1-APC target SnoN. Neuron. 2006; 50:389–400. [PubMed: 16675394]

Suliman BA, Xu D, Williams BR. The promyelocytic leukemia zinc finger protein: two decades of molecular oncology. Front Oncol. 2012; 2:74. [PubMed: 22822476]

Sun F, He Z. Neuronal intrinsic barriers for axon regeneration in the adult CNS. Curr Opin Neurobiol. 2010; 20:510–518. [PubMed: 20418094]

Sun F, Park KK, Belin S, Wang D, Lu T, Chen G, Zhang K, Yeung C, Feng G, Yankner BA, He Z. Sustained axon regeneration induced by co-deletion of PTEN and SOCS3. Nature. 2011; 480:372–375. [PubMed: 22056987]

Tanaka T, Inazu T, Yamada K, Myint Z, Keng VW, Inoue Y, Taniguchi N, Noguchi T. cDNA cloning and expression of rat homeobox gene, Hex, and functional characterization of the protein. Biochem J. 1999; 339(Pt 1):111–117. [PubMed: 10085234]

Tedeschi A, Nguyen T, Puttagunta R, Gaub P, Di Giovanni S. A p53-CBP/p300 transcription module is required for GAP-43 expression, axon outgrowth, and regeneration. Cell Death Differ. 2009; 16:543–554. [PubMed: 19057620]

Wang Z, Reynolds A, Kirry A, Nienhaus C, Blackmore MG. Overexpression of Sox11 promotes corticospinal tract regeneration after spinal injury while interfering with functional recovery. J Neurosci. 2015; 35:3139–3145. [PubMed: 25698749]

Yiu G, He Z. Glial inhibition of CNS axon regeneration. Nat Rev Neurosci. 2006; 7:617–627. [PubMed: 16858390]

Zhang F, Wang LP, Brauner M, Liewald JF, Kay K, Watzke N, Wood PG, Bamberg E, Nagel G, Gottschalk A, Deisseroth K. Multimodal fast optical interrogation of neural circuitry. Nature. 2007; 446:633–639. [PubMed: 17410168]

Zhang J, McKenna LB, Bogue CW, Kaestner KH. The diabetes gene Hhex maintains delta-cell differentiation and islet function. Genes Dev. 2014; 28:829–834. [PubMed: 24736842]

Highlights

- HHEX emerged as an axon growth inhibitor in a screen of cancer-related factors
- HHEX is expressed in adult CNS neurons but not early postnatal or DRG neurons
- Forced HHEX expression in postnatal or DRG neurons reduces axon growth
- HHEX activity depends on its transcriptional repression domain

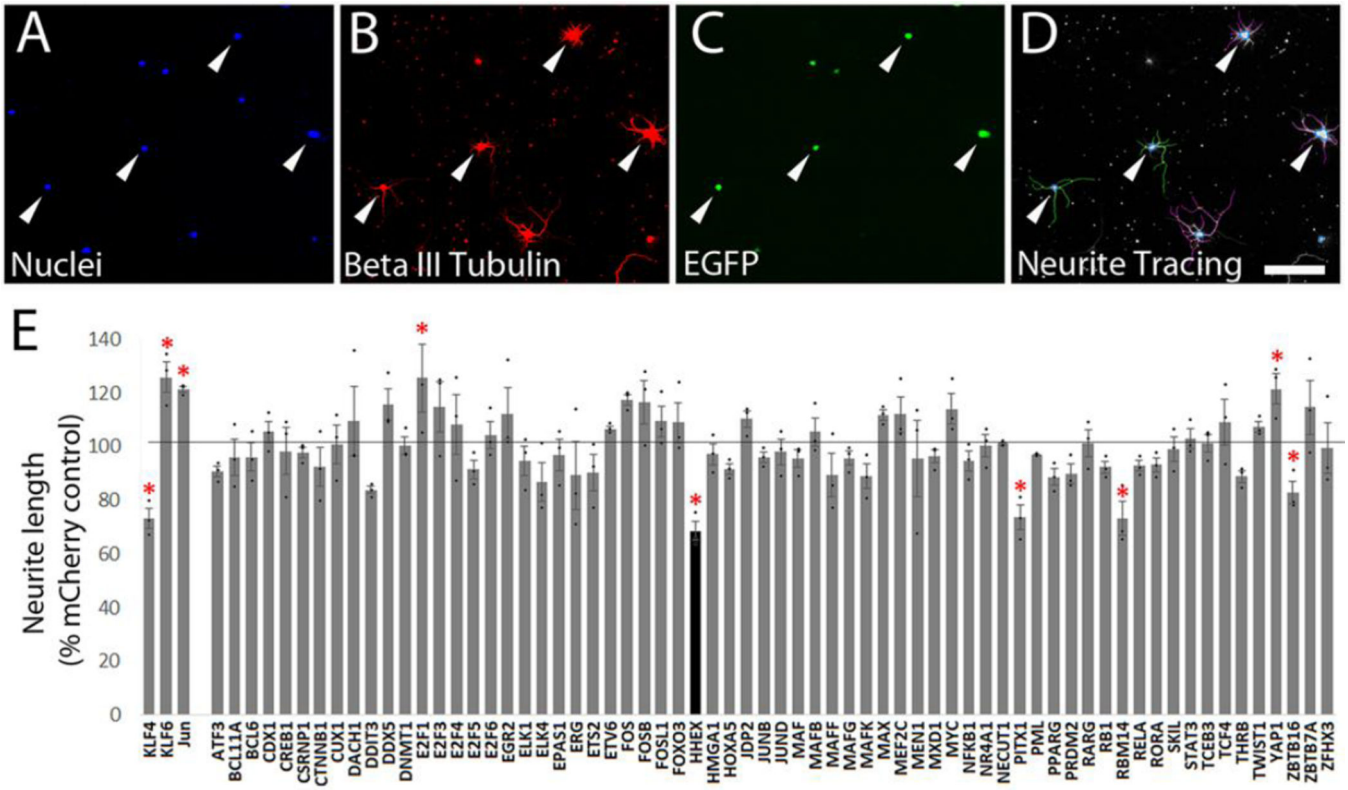

Fig 1. Phenotypic screening of oncogenic and tumor suppressive transcription factors identifies HHEX as an inhibitor of neurite outgrowth

P3 cortical neurons were co-transfected with EGFP and either mCherry control or test plasmid and cultured on laminin substrates for two days. (A–D) Images were acquired through automated microscopy (Nuclear: DAPI, Neuronal: βIII-Tubulin, Transfection: EGFP). Cells positive for neuron-specific βIII-Tubulin and EGFP (arrowheads, B and C) were used for subsequent analyses. (E) Bars show the average neurite length in cells expressing 69 test genes across three replicate experiments (dots), normalized to mCherry control. Test genes included KLF4, KLF6, and JUN, all of which showed expected changes in neurite length, confirming assay sensitivity. Six additional test genes significantly altered neurite length, two positively and four negatively. HHEX (black bar) strongly and consistently inhibits neurite outgrowth. *p<05 ANOVA with post-hoc Dunnett's, N>100 cells in three replicate experiments. Scale bar is 50μm.

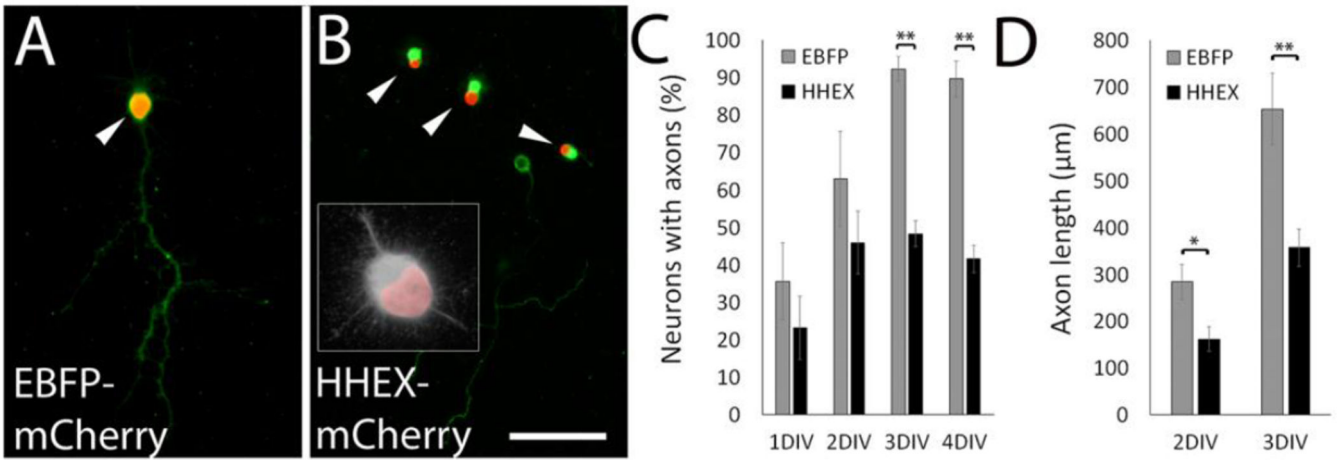

Fig 2. HHEX expression reduces axon formation and elongation

P3 cortical neurons were transfected with HHEX-2A-mCherry or EBFP-2A-mCherry control and cultured for 1 to 4 days in vitro (DIV). (A,B) Tau1 immunohistochemistry (green) identifies axons in neurons cultured for three days. Transfected neurons are identified by mCherry fluorescence (arrowheads). Neurons expressing EBFP control extended long axons, whereas neurons transfected with HHEX extended no axons or short axons (arrowheads, B, inset is HHEX phenotype in higher magnification with βIII tubulin in white). (C) Quantification of the percent of neurons with Tau1+ processes shows a significant reduction in axon differentiation in HHEX expressing cells at the 3 and 4 day timepoint. (D) Quantification of axon length, based only on neurons that possessed a Tau1+ process, shows significant reduction in HHEX-expressing neurons compared to control at 2 and 3 days in vitro. * $p<05$, ** $p<01$, paired t-test, $N>40$ cells each of three replicate experiments. Scale bar is 50µm.

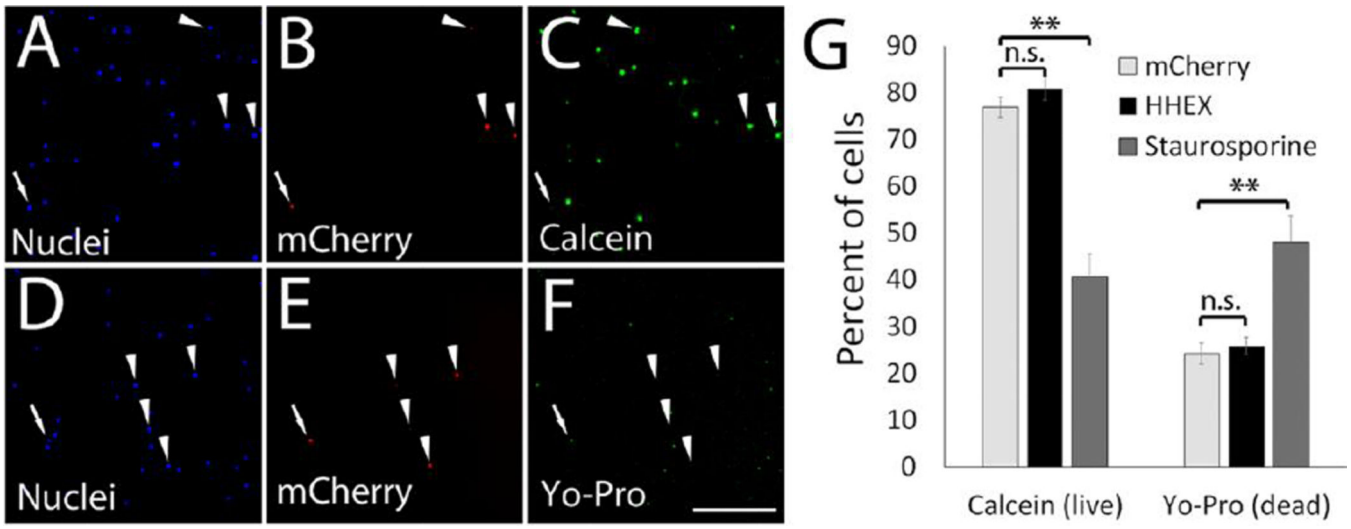

Fig 3. Cell viability is unaffected by HHEX overexpression

P3-P5 cortical neurons were transfected with HHEX or EBFP control along with mCherry reporter and cultured for two days. Staurosporine toxin was added to a subset of EBFP-transfected cells as a positive control for detection of altered viability. Cells were visualized with DAPI (A, D), mCherry reporter (B, E), and live cell indicator calcein (C) or the dead cell indicator Yo-Pro (F). Arrowheads indicate nuclei (DAPI, A and D) associated with transfected cells (mCherry positive, B and E) that are alive (positive for calcein, C, or negative for Yo-Pro, F). (G) Quantification based on cellomics automated microscopy shows that staurosporine significantly reduces the percent of calcein-positive cells and increases the percent of Yo-Pro positive cells, whereas HHEX expression had no effect. **p<01, n.s. p>05, Anova with post-hoc Dunnett's. N>200 transfected cells from each of six replicate experiments. Scale bar is 50μm.

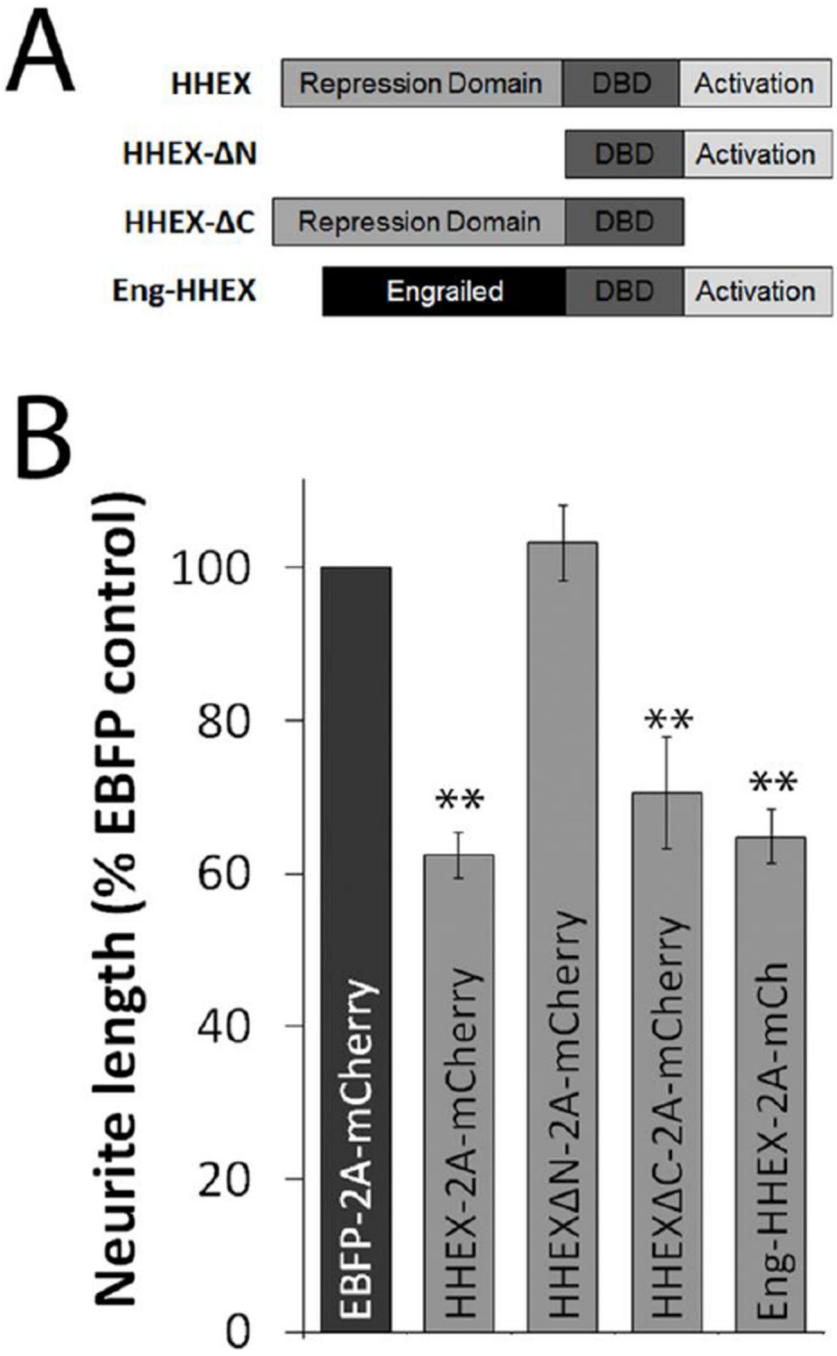

Fig 4. A transcriptional repression domain is both necessary and sufficient for HHEX's inhibition of neurite growth

Domain-deletion and domain-swapped HHEX mutants, shown schematically in (A), or EBFP control plasmids were overexpressed in early postnatal cortical neurons and cultured for two days. (B) Neurite outgrowth was quantified by automated microscopy. HHEX-ΔC inhibits neurite growth similarly to full length HHEX, showing that the C-terminal activation domain is dispensable for growth inhibition. In contrast, removal of the N-terminal domain abolished growth inhibition. Finally, Engrailed-HHEX also inhibits neurite growth. These experiments suggest that HHEX likely inhibits neurite outgrowth through a mechanism of

transcriptional repression. ** p<01, ANOVA with post-hoc Dunnett's. N>150 transfected cells in each of five replicate experiments.

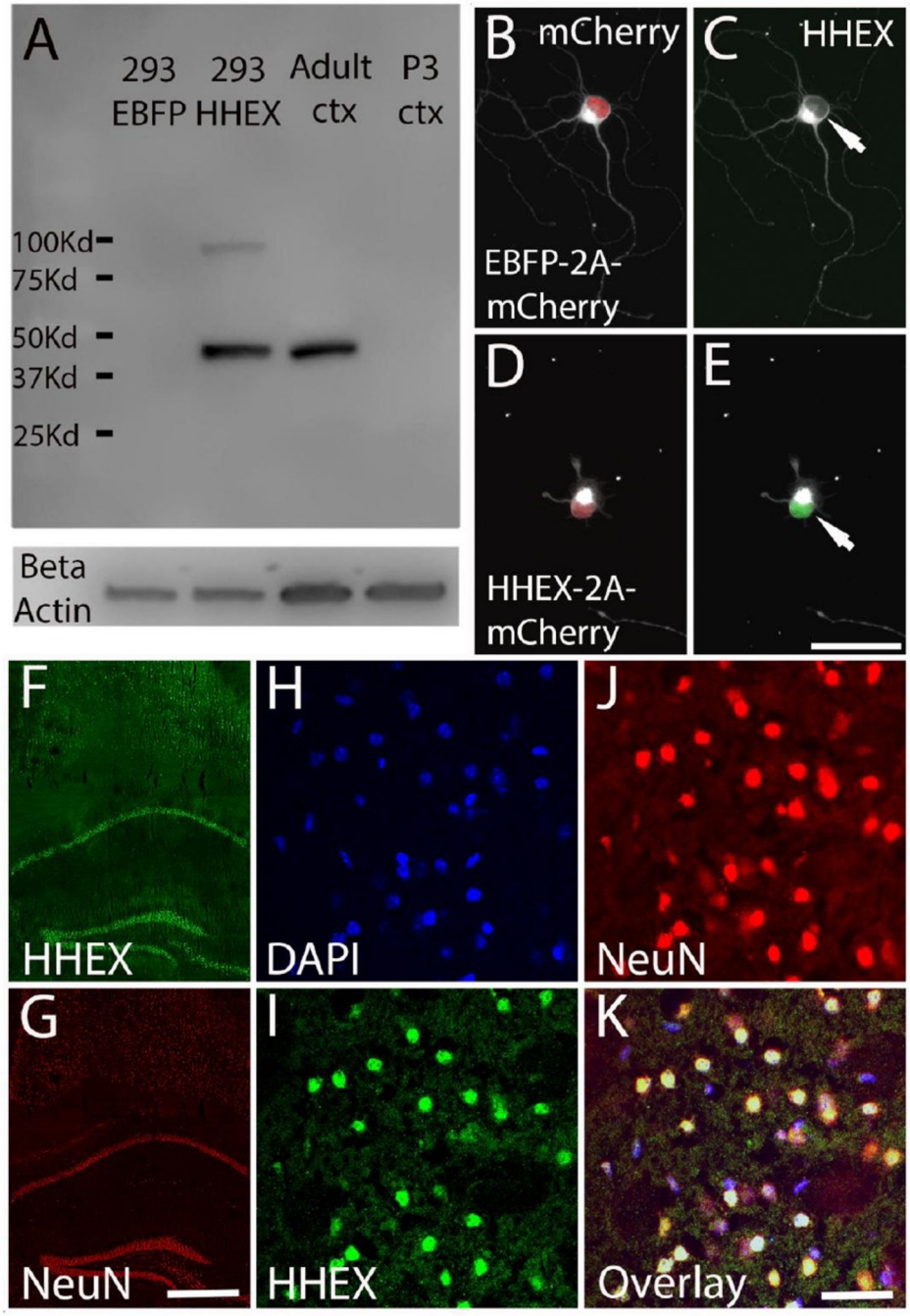

Fig 5. HHEX is widely expressed in adult, but not neonatal, CNS neurons

(A) Western blotting detects HHEX in 293 cells transfected with HHEX plasmid, but not in EBFP-transfected control cells, confirming antibody specificity. HHEX protein is also detected in adult murine cortex, but not in postnatal tissue at the age used to prepare neurons for cell culture. (B–E) P3 cortical neurons were transfected with EBFP-2A-H2B-mCherry control plasmid or HHEX-2A-H2B-mCherry and cultured for two days. mCherry expression (red, B,D) identifies transfected cells, and immunohistochemistry for βIII tubulin (white) identifies neurons. Immunohistochemistry detects HHEX in HHEX-transfected neurons

(green, arrow, E), but not in control transfected neurons (arrow, C). Adult hippocampus (F,G) or cortex (H–K) was stained with DAPI (nuclei, H), anti-NeuN antibody (J,G) and anti-HHEX antibody (F,I). In both brain regions, endogenous HHEX expression co-localized with NeuN confirming widespread expression of HHEX in neuronal nuclei in the CNS. Scale bars are 50μm (E), 500μm (I), and 20μm (K).

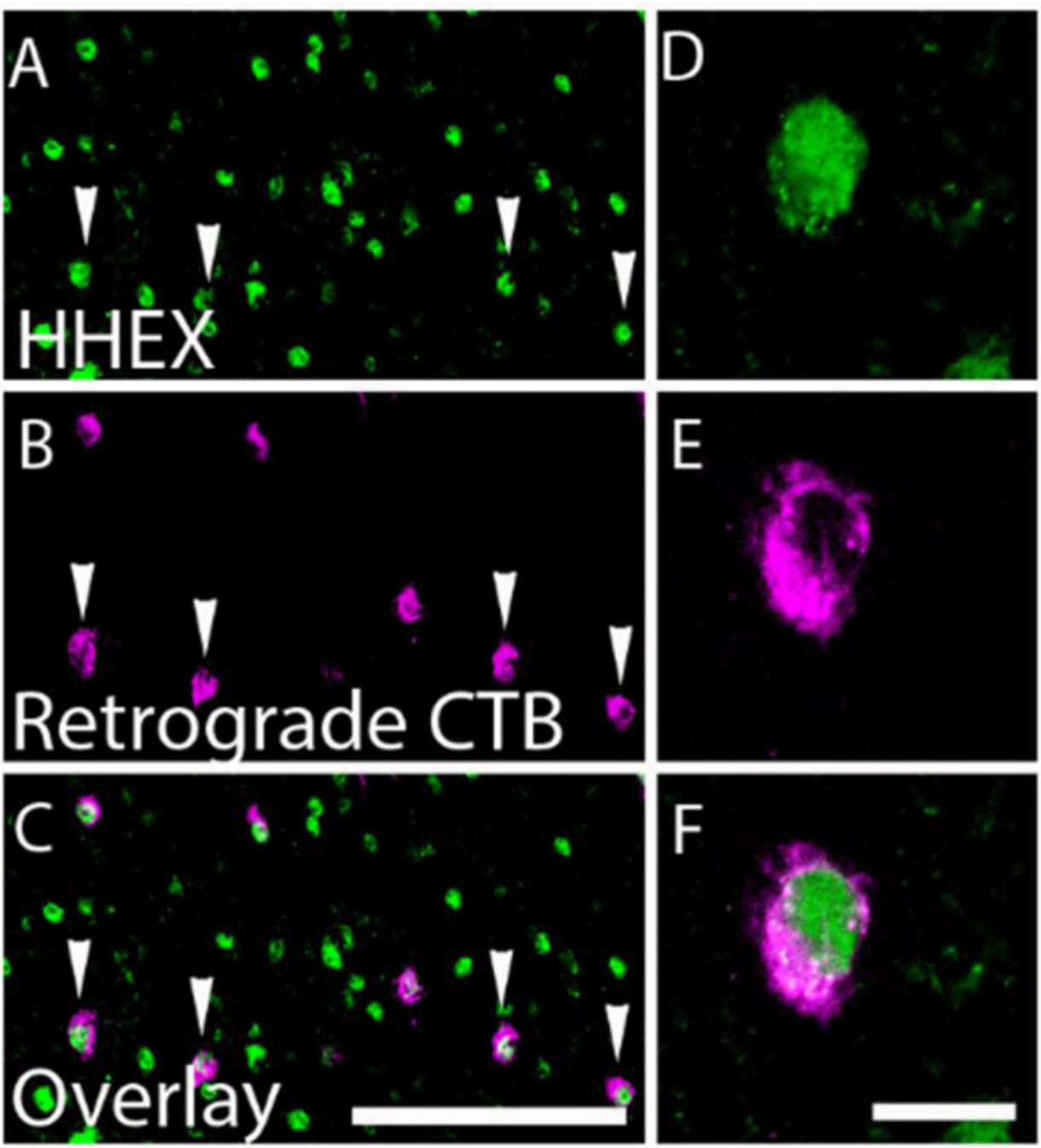

Fig 6. HHEX is expressed in corticospinal tract (CST) neurons after axotomy

CST axons were severed in the cervical spinal cord of adult mice and the retrograde tracer cholera toxin B (CTB) conjugated to Alexafluor 647 (CTB-647) injected to the injury site. Two weeks later cortical sections were prepared and immunohistochemistry for HHEX performed. (A,D) show HHEX expression, (B, E) show retrogradely identified CST neurons, and (C,F) show the overlap. Arrows indicate CST neurons with clear HHEX signal. Scale bars are 100μm (C) and 10μm (F).

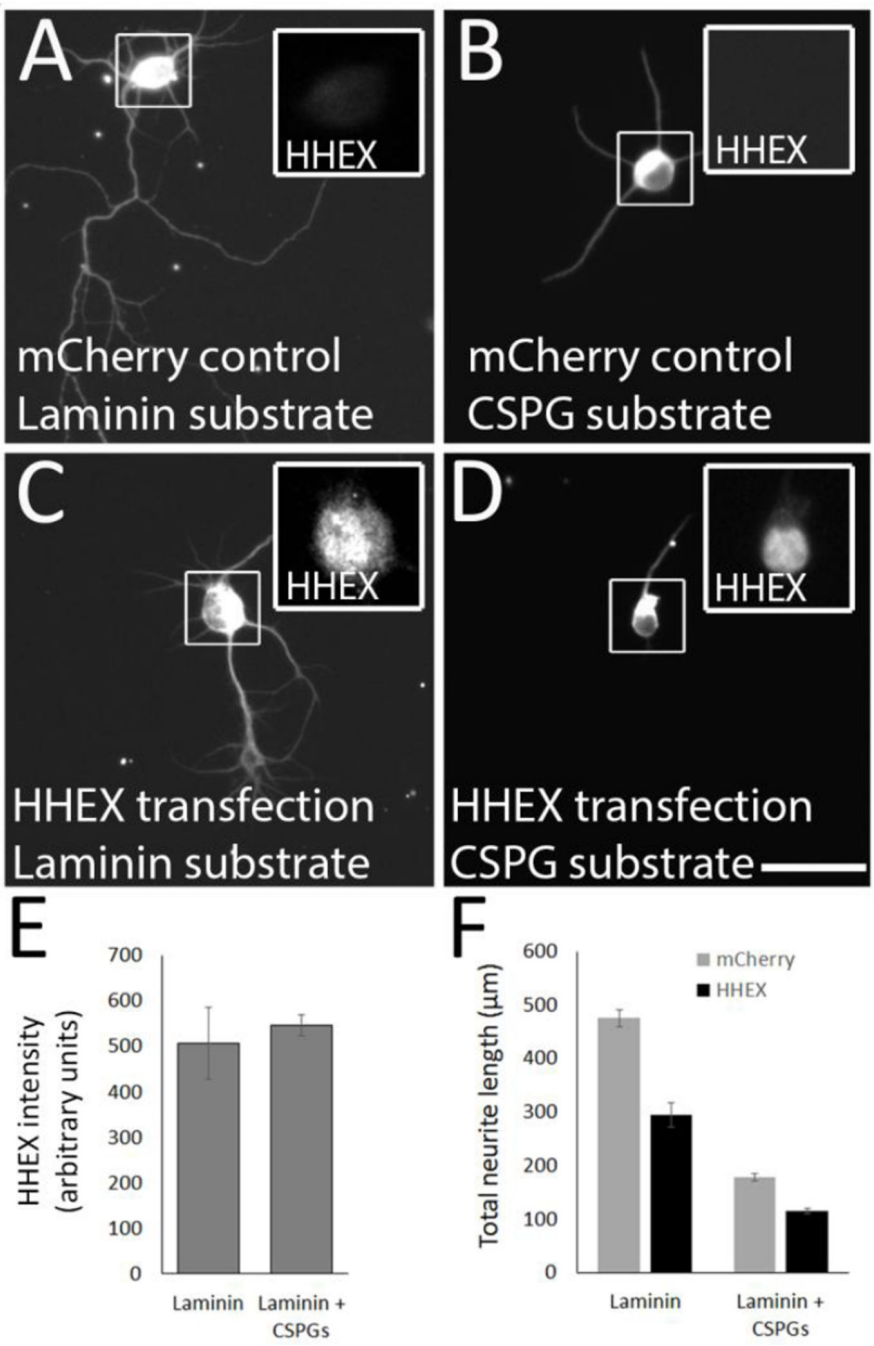

Fig 7. HHEX inhibits neurite outgrowth independently of chondroitin sulfate proteoglycan signaling

Cortical neurons were transfected with EBFP control plasmid or HHEX and cultured for three days on laminin or a laminin/CSPG mixture. Automated image analysis quantified the intensity of HHEX immunohistochemistry and the length of neurites. (A–D) HHEX protein was not detected EBFP-transfected neurons on laminin (inset, A) or CSPG (inset, B) substrate, but was readily visible in HHEX-transfected neurons (insets, C,D). (E) Quantification of HHEX immunohistochemistry performed on untransfected neurons shows no significant change in HHEX expression as a result of exposure to CSPG substrates (p>05,

paired t-test, N>2000 neurons). (F) Neurite lengths were significantly reduced on CSPG substrates. On both laminin and CSPG substrates, transfection with HHEX plasmids decreased neurite lengths compared to EBFP control. **P<01, two way ANOVA, N>100. Scale bar is 10μm.

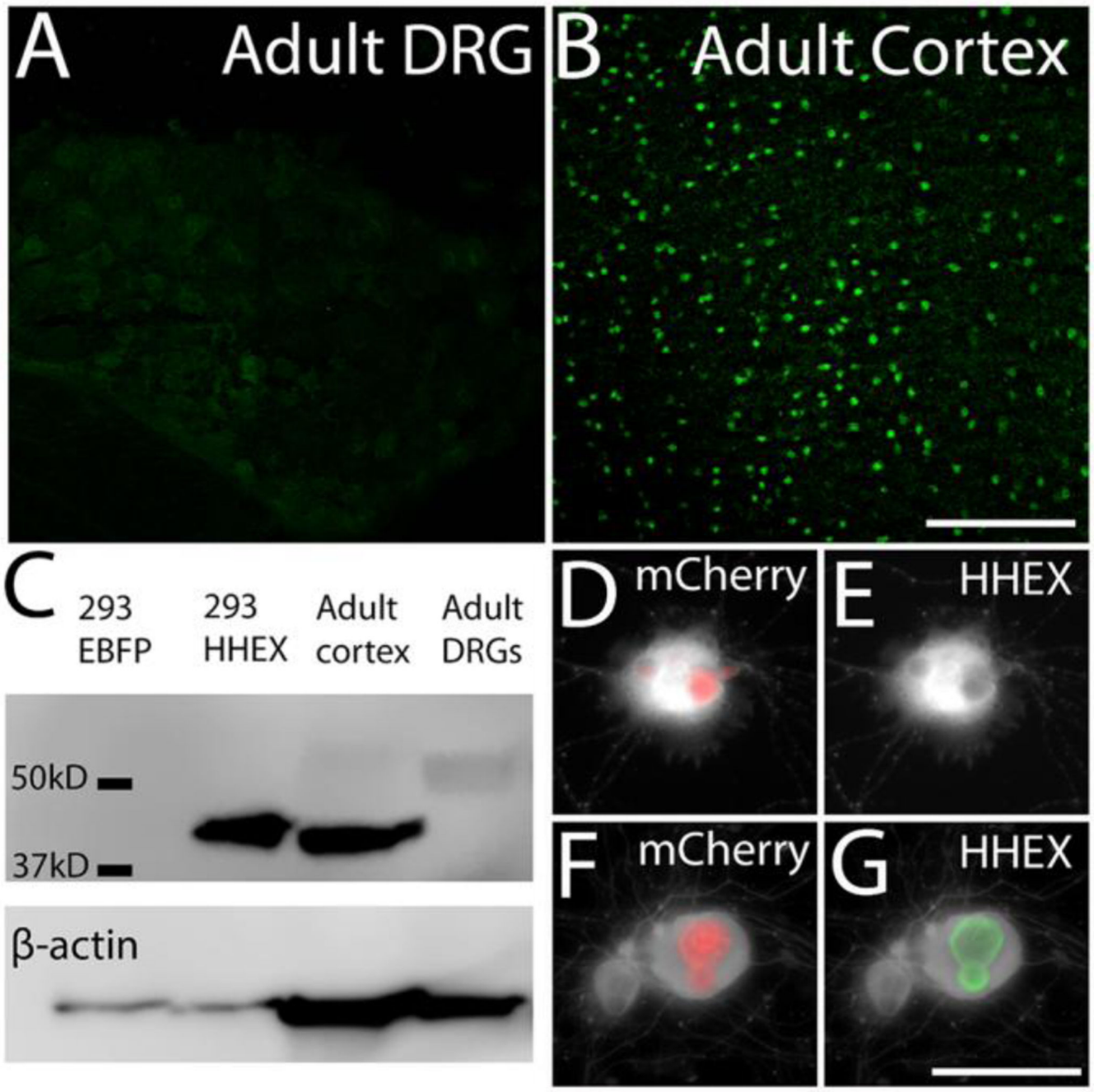

Fig 8. HHEX is more abundant in central than in peripheral nervous system

(A,B) Dorsal root ganglia (DRG, A) and cortex (B) were stained in parallel with anti-HHEX antibodies. HHEX is readily detectable in cortex but, using identical acquisition parameters, was not detected in DRG tissue. (C) Western blotting detects HHEX protein in HHEX-transfected 293 cells and adult cortex, but detects only faint and size-shifted protein bands in DRG tissue. (D–G) Adult DRG neurons were transfected with control EBFP-2A-H2B-mCherry (D,E) or HHEX-2A-H2B-mCherry (F,G), cultured on laminin substrate for four days, followed by immunohistochemistry for βIII tubulin (white) and HHEX (green, E,G).

HHEX was not detected in EBFP-transfected DRG neurons, but was readily detected in HHEX-transfected cells. Scale bars are 100μm (A) and 50μm (D–G).

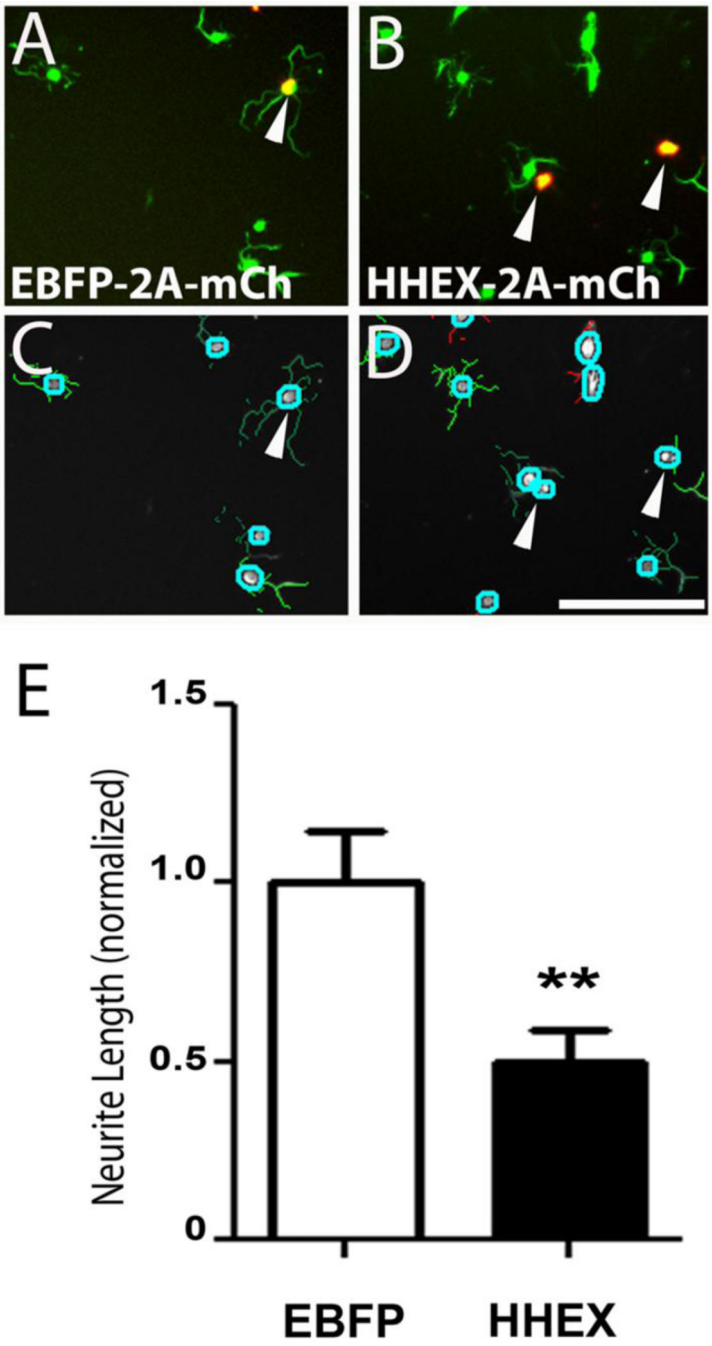

Fig 9. HHEX overexpression reduces DRG neurite outgrowth

Adult DRG neurons were transfect with EBFP-2A-H2B-mCherry (A, C) or HHEX-2A-H2B-mCherry (B,D), maintained for three days, re-plated to remove existing neurites, and then maintained for one additional day. Neuron-specific tubulin (green, A,B) identifies neurites and mCherry (arrowheads, A,B) identifies transfected cells. (C,D) Neurite outgrowth was quantified with the Neuronal Profiling Algorithm on a Cellomics ArrayScanXTI High Content Analysis microscope (ThermoFisher) after imaging and mask creation. Cell bodies are indicated by blue circles, and neurites are shown in green or red.

(E) Neurite outgrowth was normalized to the average total neurite length for EBFP-2A-H2B-mCherry transfected DRGs. N>100 cells in three replicate experiments, ** $p<0.001$, Paired t-test. Scale bar is 150μm.